

**Role of the self-interaction error in studying chemisorption on graphene from first-principles**Simone Casolo,<sup>1,\*</sup> Espen Flage-Larsen,<sup>2</sup> Ole Martin Løvvik,<sup>2,3</sup> George R. Darling,<sup>4</sup> and Gian Franco Tantardini<sup>1,5</sup><sup>1</sup>*Dipartimento di Chimica Fisica ed Elettrochimica, Università degli Studi di Milano, via Golgi 19, 20133 Milan, Italy*<sup>2</sup>*Department of Physics, University of Oslo, P.O. Box 1048, Blindern, NO-0316 Oslo, Norway*<sup>3</sup>*SINTEF, Materials and Chemistry, Forskningsvn., NO-0314 Oslo, Norway*<sup>4</sup>*Surface Science Research Centre, Department of Chemistry, The University of Liverpool, Liverpool L69 7ZD, United Kingdom*<sup>5</sup>*CIMAINA, Interdisciplinary Center of Nanostructured Materials and Interfaces, University of Milan, via Golgi 19, 20133 Milan, Italy*

(Received 25 February 2010; revised manuscript received 15 April 2010; published 10 May 2010)

Adsorption of gaseous species, and in particular of hydrogen atoms, on graphene is an important process for the chemistry of this material. At the equilibrium geometry, the H atom is covalently bonded to a carbon that puckers out from the surface plane. Nevertheless the *flat* graphene geometry becomes important when considering the full sticking dynamics. Here we show that GGA-DFT predicts the wrong spin state for this geometry, namely,  $S_z=0$  for a single H atom on graphene. We show that this is caused by fractional electron occupations in the two bands closest to the Fermi energy, an effect of the self-interaction error. It is also demonstrated that the use of hybrid functionals or the GGA+ $U$  method can be used to retrieve the correct spin solution although the latter gives an incorrect potential energy curve.

DOI: [10.1103/PhysRevB.81.205412](https://doi.org/10.1103/PhysRevB.81.205412)

PACS number(s): 73.22.Pr, 71.15.Mb

**I. INTRODUCTION**

Due to its peculiar semimetallic band structure, graphene is a very promising material for future silicon-free nanoelectronics.<sup>1,2</sup> In particular, graphene's charge-carriers mobility is extraordinarily high, with mean-free paths in the order of microns.<sup>3,4</sup> However, for the fabrication of logic devices the absence of a band gap is a major issue since it does not allow a complete current turn-off, hence high on-off ratios.<sup>2,5</sup>

One straightforward possibility for band-gap engineering of graphene is to adsorb radicals or small molecules to create  $\pi$  defects, breaking the equivalence of its two sublattices. Previous studies, mostly based on density functional theory (DFT), have computed adsorption energies and geometries of isolated,<sup>6,7</sup> clustered,<sup>8–11</sup> and even superlattices of adsorbates on graphene, with studies of hydrogen atom adsorption predominating.

The interaction of hydrogen with carbon based materials and its sticking dynamics has already been the object of several studies because it has important implications in several fields. Among these, are hydrogen storage materials,<sup>12</sup> the erosion process of graphite lining in nuclear fusion reactors,<sup>13</sup> and the recombination reaction to form H<sub>2</sub> in the interstellar medium catalyzed by carbonaceous dust grains.<sup>14,15</sup>

However, hydrogen chemisorption dynamics on graphene is not yet completely understood. In the adiabatic picture when an H atom impinges on graphene and binds at its top site it induces one carbon atom to move out from the plane, “puckering” the surface. On the other hand, if the incoming species moves fast enough toward the graphene layer, sticking can occur faster than surface reconstruction; in this case the substrate can be considered to be rigid. The planar geometry may thus play an important role in the adsorption dynamics, and it has to be considered in computing accurate potential energy surfaces for dynamical studies.

In this article we analyze the first-principles spin properties of the substrate when a hydrogen atom chemisorbs on a

*flat* and rigid graphene sheet. We show that the loss of spin polarization is fictitious, deriving from the self-interaction error in semilocal generalized gradient approximation (GGA) functionals. We also show that the correct ground state magnetization can be achieved using a hybrid functional or the GGA+ $U$  approach, although the latter fails to reproduce the correct H-graphene potential energy curve.

**II. COMPUTATIONAL METHODS**

Periodic density functional theory as implemented in the VASP package<sup>16,17</sup> has been used throughout. A GGA-Perdew-Burke-Ernzerhof (PBE) functional<sup>18</sup> was used and the plane wave basis set was limited to a 500 eV energy cutoff. For the inner electrons we rely on the frozen core approximation using projector-augmented wave (PAW) pseudopotentials.<sup>19,20</sup>

The reciprocal space was sampled by  $\Gamma$  centered  $k$ -point grids, whose meshes were chosen depending on the supercell size, but never sparser than  $6 \times 6 \times 1$ . The graphene unit supercells used here range from a  $2 \times 2$  to a  $5 \times 5$ : all of them have a vacuum region along the  $c$  axis of 20 Å in order to guarantee a vanishing interaction between periodically repeated images.

It has been shown recently that for hydrogen adsorption a  $5 \times 5$  supercell is still not large enough to extract adsorption energies at meV accuracy,<sup>8</sup> although this goes beyond the aim of this work. Further details about the computational setup can be found in Ref. 8.

**III. RESULTS AND DISCUSSION**

When a radical species chemisorbs onto graphene or graphite the most favorable outcome is the formation of a covalent bond with one of the surface carbons, i.e., at a top site. The simplest radical is a single (neutral) hydrogen atom. It is known that as H approaches the substrate plane interacts with a  $\pi$  electron of graphene, triggering orbital rehybridiza-

tion of a C atom from a planar  $sp^2$  to a partially tetrahedral  $sp^3$  configuration. When the graphene sheet is allowed to reconstruct it puckers, with the rehybridized C atom pulled out 0.6 Å from the layer plane.<sup>6,7</sup>

Recent valence bond (VB) calculations of the different spin manifolds arising from the 1s and six  $\pi$  electrons of a H-benzene test system, gave some more insight on this process. Indeed, at long range, the adsorbate-substrate interaction is purely repulsive since there is no unpaired electron available on (singlet) graphene to bind with the (doublet) hydrogen. At short range, however, a low-lying excited (triplet) spin state exists in graphene, where two  $\pi$  electrons lying on opposite, nonoverlapping ends of a benzene ring would give rise to an attractive, barrierless interaction with the H 1s lone electron. Hence, an avoided crossing occurs between these two overall doublet curves giving rise to an activation barrier to chemisorption (see Fig. 5 in Ref. 8).

The graphene lattice is a bipartite system, made of two equivalent  $\pi$  orbital sublattices, located on alternating carbon atoms. The equivalence of the two honeycomb sublattices is responsible for the particle-hole symmetry in graphene, and for the peculiar conical intersection between the valence and conduction bands at  $E_F$ .<sup>21</sup> A chemisorbed species creates a defect in the aromatic network, hence an imbalance between the number of occupied sites of the two  $\pi$  sublattices ( $n_A$  and  $n_B$ , respectively). According to a theorem formulated by Inui *et al.* within tight-binding theory, whenever an imbalance (vacancy) is introduced in a bipartite lattice this gives rise to  $|n_A - n_B|$  zero-energy midgap states, localized on one sublattice only.<sup>22</sup> Moreover, following Lieb's second theorem,<sup>23</sup> since the total number of electrons is odd the total magnetization for nonmetallic systems has to be  $S = |n_A - n_B|/2$ . Thus, for a single defect  $S_z = 1/2$ , or  $1 \mu_B$ .

DFT calculations confirm this picture: the hydrogen atom introduces a  $\pi$  defect in one of the two sublattices, breaking one of the many aromatic bonds around the tetrahedral carbon. This implies that an unpaired electron on one sublattice can be delocalized by a "bond switching" process along the other sublattice. In the energy spectrum this results in a flat band at the Fermi level, i.e., in a midgap state occupied by one single spin projection only.<sup>8,24</sup>

In previous studies<sup>6,7</sup> it was found that, at the GGA-DFT level, keeping the substrate planar thwarts the  $sp^2$ - $sp^3$  rehybridization. This weakens the attractive C-H interaction, and it is enough to corrupt the system's aromatic character. Nevertheless, because the VB arguments concerning the crossing of two spin states hold, a metastable C-H bond can form.

From our DFT calculations we observed that the total spin for H adsorbed on flat graphene is lower than expected at the local minimum geometry. In Fig. 1 is shown the magnetization (left panel) along the adsorption path,  $z_H$ , for several surface coverages, together with the total energies for the spin-polarized and unpolarized solutions (right panel). When the radical is far from the surface, its magnetic moment is correctly  $1 \mu_B$ : this corresponds to an electron lying in the H 1s orbital, while the graphene electronic structure remains intact. As the atom approaches the graphene layer along the normal direction, at a given critical height from the surface ( $z_c \approx 1.25$  Å) the system's spin drops. The minimum value for the total spin depends upon the coverage. If the coverage

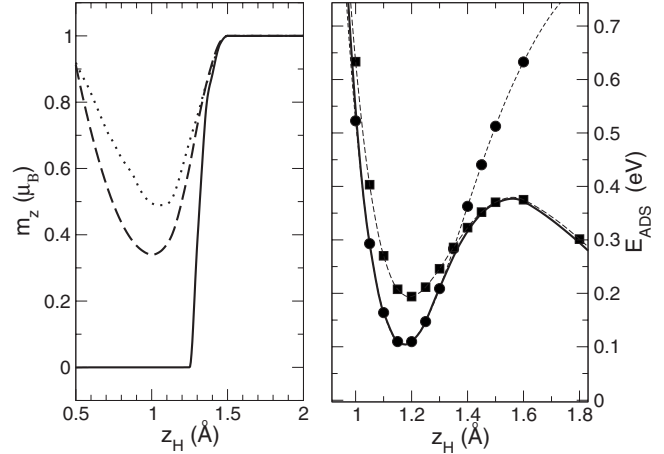


FIG. 1. Left panel: total spin vs distance from the surface for a H atom adsorbing on flat graphene. The coverages are the following:  $\Theta = 0.031$  (full line),  $0.055$  (dashed) and  $0.125$  ML (dotted). Right panel: H adsorption potential curves at  $\Theta = 0.031$  ML (full line) together with the same curves for the spin unpolarized case (squares) and for the fixed magnetization  $1 \mu_B$  (circles). The full line shows the adiabatic (polarized and nonconstrained) curve. Zero energy here is set for H asymptotically far from the graphene.

is low enough the spin is eventually quenched down to zero. On pushing the adsorbate closer to the carbon atom the magnetization tends to increase again. We tested that the same picture also holds for other small organic radicals (methyl and ethyl) with slightly different critical heights, weakly dependent upon the supercell size (coverage).

When comparing the adsorption curves computed with a magnetization fixed at either 0 (nonpolarized DFT) or  $1 \mu_B$  as shown in the right panel of Fig. 1, it is clear that the nonpolarized solution becomes more stable than the magnetic one for  $z_H < z_c$ .

On closer inspection [see Fig. 2(b)] we see that the occupied hydrogen  $s$  orbital and its (empty) affinity level get closer in energy when approaching graphene, consistent with the Newns-Anderson model.<sup>25,26</sup> Then around  $z_c$  they approach the Fermi energy ( $E_F$ ), become degenerate and equally occupied by a fractional number of electrons. In the density of states, a gap opens at the point of the spin quenching together with the formation of a broad partially occupied peak at  $E_F$ , symmetric for both spin projections.

If the host were a metal, then spin-flip scattering between conduction electrons and a magnetic impurity might lead to a singlet ground state (the Kondo effect). Although DFT does not describe the Kondo effect well, it can describe correctly the spin quenching of an H atom impinging on metallic substrates such as Cu, Ag, or Al (where the spin transition has been interpreted as a signature of nonadiabatic effects) if the magnetization is constrained.<sup>27,28</sup> However in our case there is no delocalized free-electron-gas-like surface state (a Shockley state) that is free to screen the impurity. Moreover the  $s$  electron does not belong to a localized orbital decoupled from the substrate such as for  $d$  metals.

In the absence of metallic screening, our results indicate that radical adsorption on planar graphene is a situation in which the many-electron self-interaction error (SIE, also

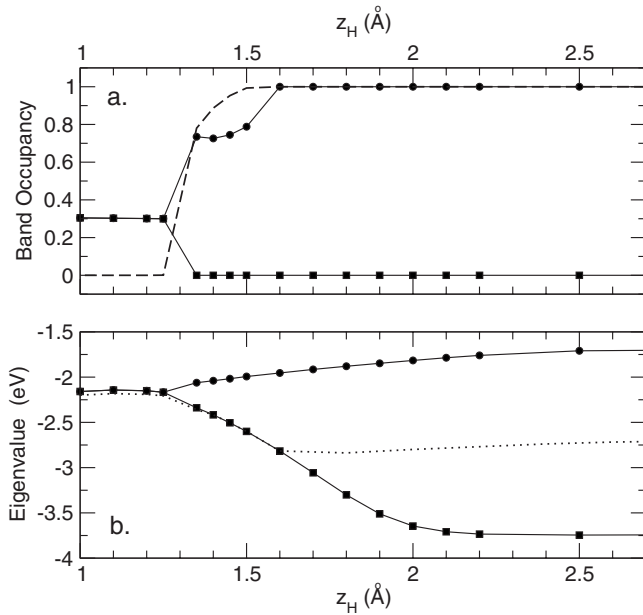


FIG. 2. (a): Occupancy for the spin up (circles) and spin down (squares) bands closest to  $E_F$  along the whole adsorption path. Dashed line: total magnetization (in  $\mu_B$ ). (b): Eigenvalues for the bands shown above, the dotted line represents the value of the Fermi energy.

known as delocalization error)<sup>29</sup> is particularly severe. Following the notation in Ref. 30 this is a chemical reaction with two centers ( $m=2$ ) and one electron ( $n=1$ ), since none of the electrons of graphene may be directly involved in bonding if they cannot rehybridize to a tetrahedral  $sp^3$  state. Systems with a fractional  $n/m$  ratio are known to suffer from the SIE and also to exhibit large static electronic correlation.<sup>31</sup>

A well known system with  $n/m=1/2$  is the dissociation of the  $H_2^+$  molecular ion. When the two atoms are far apart both the local density approximation (LDA) and GGA local functionals give as the ground state half of an electron on each of atomic fragments, which is physically incorrect. Asymptotically the orbitals on the two fragments are degenerate, so this fractional occupation solution should be degenerate with any other possible electronic arrangement such as one filled and one empty orbital.<sup>32</sup> Fractional charge (and spin) on the two fragments is due to the delocalization that is a direct consequence of the SIE. Indeed the LDA and GGA functionals are designed to correctly reproduce the system's total density and the on-top pair density, but fail in pathological systems to reproduce spin densities.<sup>33,34</sup> The SIE induces the breakdown of sum rules over the exchange hole density that results in a convex behavior of the total energy for a fractional orbital occupation instead of the usual linear tendency predicted by Janak's theorem.<sup>35</sup> Hence, for open systems a delocalized situation with fractional charge turns out to be more favored.<sup>29</sup>

For H adsorbed on flat graphene the spin quenching is similarly due to a fractional spin situation: the "splitting" of one electron in two different *degenerate* bands (originating from H  $s$  and C  $p_z$ ), with opposite spin projections (see Fig. 2). Here the occupation numbers in these bands can fluctuate,

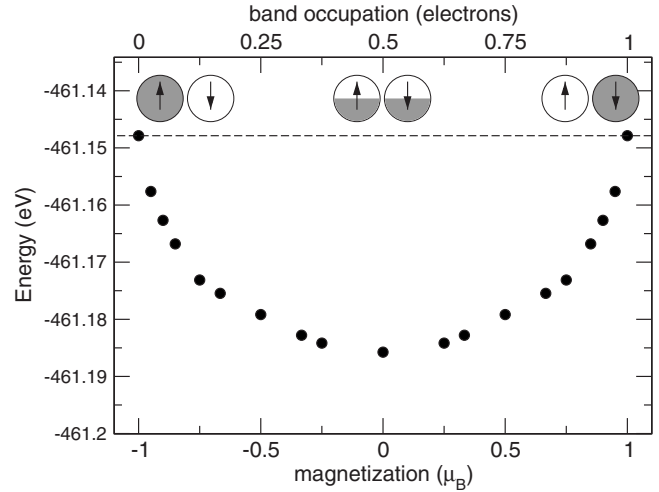


FIG. 3. Calculated total energy vs magnetization for one H atom adsorbed on flat graphene. When the magnetization is  $-1$  or  $1 \mu_B$  one of the two degenerate bands is occupied while the other is empty. For the nonpolarized,  $0 \mu_B$ , case both bands are occupied by half of an electron each. The dashed line represents the correct degenerate behavior for fractional electron numbers; filled circles are the GGA-DFT results.

a sign that SIE is particularly severe.<sup>36</sup> This picture is confirmed by the convex behavior of the system energy for fractional band occupation as shown in Fig. 3, obtained by constraining a given occupation within the two bands. Note that in the case of two degenerate orbitals every arrangement of electrons (even for fractional occupations) should be perfectly degenerate. In this case however, the energy minimum lies exactly at the unpolarized solution: 0.5 occupancy of the two bands.

A further indication of the SIE is the worsening of the spin quenching at low coverages, i.e., for larger and larger super cells, as shown before in Fig. 1. With the SIE causing delocalization, the fractional occupancy might not be optimal when the unit cell is not large enough to accommodate all the delocalized electron density.<sup>37</sup>

A major difference with the  $H_2^+$  prototype case is that here there is no fractional spin asymptotically for H since the orbitals involved here lie far from graphene Fermi energy. For more electronegative monovalent species, such as F and OH, fractional charges do appear also asymptotically. This is similar to dissociation of heteronuclear diatomics,<sup>38</sup> in this case the affinity level of F and OH lie below the Fermi energy of graphene, so it gets partially filled.

To prove further that the failure in representing the total spin of the system comes from the approximate nature of the density functionals, we tested the performance of a (nonlocal) hybrid functional. Hybrid functionals combine the GGA exchange and correlation term (convex for fractional electron number) with the Hartree-Fock (HF) "exact" exchange term. Since HF energies have instead a strong concave behavior for fractional electron numbers they often yield overcorrected results.<sup>37</sup> For this reason the use of a fraction (usually one fourth) of exact exchange to correct the  $E_{xc}$  functional gives much better results, at least for nonmetallic systems.<sup>39</sup> We chose the PBE0 functional, which mixes 25% of HF with

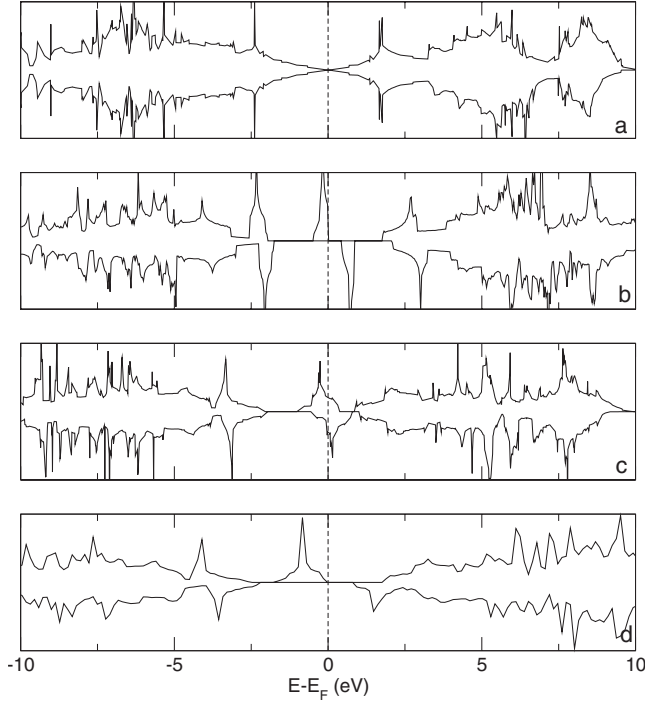


FIG. 4. Density of states for the H-flat graphene system obtained for a  $2 \times 2$  supercell. PBE results for: (a) clean graphene, (b) H adsorbed on reconstructed (puckered) graphene, (c) H adsorbed on flat graphene ( $M=0 \mu_B$ ). Hybrid-PBE0 results ( $1 \mu_B$ ) are shown in (d) for comparison. As a guide to the eye the Fermi energy is shown as dashed vertical line.

75% of PBE exchange, and uses full PBE correlation<sup>40</sup>

$$E_{xc}^{\text{PBE0}} = E_{xc}^{\text{PBE}} + \frac{1}{4}(E_x^{\text{HF}} - E_x^{\text{PBE}}) \quad (1)$$

Hybrid functionals are orbital dependent, i.e., nonlocal in space. This is a major issue when employing plane wave codes where the number of orbitals depends upon the supercell volume. The computational effort needed for this kind of calculation is thus much larger compared to a GGA, and makes the study of the full potential curve extremely demanding. For this reason we had to restrict our study to a single ionic geometry, and to a  $2 \times 2$  supercell ( $\Theta=0.125$  ML).

Within hybrid functional DFT the system's total spin for H on a flat graphene layer is  $1 \mu_B$  ( $S_z=1/2$ ), and the associated spin density is correctly localized on one sublattice only. A comparison between the density of states computed with PBE and PBE0 is shown in Fig. 4. GGA can represent reasonably well the adiabatic chemisorption mechanism, namely, the band-gap opening and the zero-energy midgap state that splits by the exchange interaction into filled and empty states with opposite spins [Figs. 4(a) and 4(b)] when graphene is allowed to pucker. For the flat geometry, GGA gives a broad feature straddling the Fermi energy [Fig. 4(c)]. For larger supercells (at lower coverages) the peaks become fully symmetric for the two spin projections, giving rise to an unpolarized state. In contrast, PBE0 can reproduce well the occupied midgap state. It is widely known that standard DFT

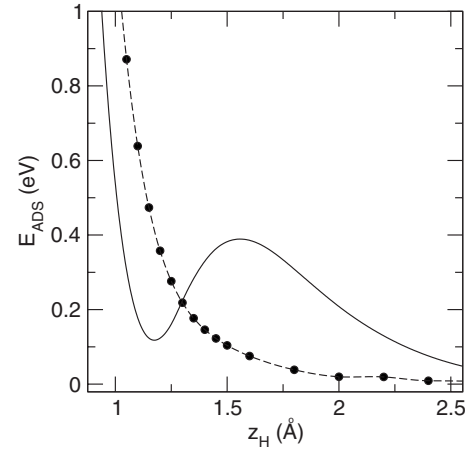


FIG. 5. Comparison between GGA (full line) and GGA+ $U$  (dashed line) potential energy curves along the adsorption path. Note how GGA+ $U$  does not show the correct activation barrier arising from the avoided crossing of the two curves shown in the right panel of Fig. 1.

tends to underestimate the band gaps, again due to the SIE.<sup>41</sup> Here we find that the PBE0 band gap is about 50% larger than that of PBE.

It has also been proposed that an on site repulsion term such as in the LDA+ $U$  (Ref. 42) approach can help to control the SIE in cases of fractional occupation.<sup>43</sup> The on-site Coulomb term  $U$  acts as a penalty for the occupation of carbon  $p$  orbitals, splitting the two degenerate bands at the Fermi energy, and thus reproducing the correct ground state magnetization. Note that LDA+ $U$  and GGA(PBE)+ $U$  give practically identical results in this case. This approach is much less computationally expensive than the hybrid functionals, so we could study the full adsorption path. As for PBE0 the total magnetization is  $1 \mu_B$  at every C-H distance, and the spin density is correctly localized either on the H atom or on one graphene sublattice. From our tests a Coulomb interaction of 15 eV was enough to retrieve the correct ground state spin: a value not far from 20.08 eV, already successfully used to describe carbon  $\pi$  electrons in similar approaches.<sup>44,45</sup>

We would like to stress that the GGA+ $U$  approach is not a rigorous way to avoid self interaction, and hence some care has to be taken when interpreting these results. While it is relatively easy to predict the correct total spin of the system from physical arguments, it is more challenging to judge the quality of total energies. Indeed, it can be seen from Fig. 5 that the effect of the on-site term,  $U$ , is to lower the activation barrier at  $z_c$  making the adsorption a fully repulsive interaction. Since the chemisorption of H on graphene results from the interplay of attractive and repulsive states of doublet spin, there must be an avoided crossing which is not evident from Fig. 5. Thus, although the GGA+ $U$  method obtains the correct magnetization, it does not correctly represent all the aspects of the H-graphene interaction.

#### IV. CONCLUSIONS

The chemisorption of a hydrogen atom onto a flat graphene sheet has been studied within semilocal GGA-DFT.

Our results show that first-principles studies of chemisorption on graphene may suffer from severe errors for this particular ionic arrangement.

In an adiabatic picture, an H atom binds covalently to an  $sp^3$  carbon puckered out from the sheet, leaving an electron localized on the lattice. The system magnetization is then  $1 \mu_B$ . Contrary to the adiabatic case, when the graphene is constrained to be flat, the substrate  $sp^2$ - $sp^3$  rehybridization is limited. Thus, within the GGA approach, adsorbate and substrate bands become degenerate at a given critical C-H distance,  $z_c$ , where the total magnetization drops to zero. This spin transition is due to a fractional spin configuration: a fictitious effect induced by the self-interaction error. To overcome this issue it is possible to use a hybrid functional such as PBE0. The GGA+ $U$  approach can also reproduce the correct magnetization, but it leads to qualitatively incorrect potential energy curves.

These results suggest that similar problems may affect other  $sp^2$  systems such as nanotubes, fullerenes and graphite whenever the rehybridization necessary in the chemisorption process cannot occur fully. In these cases a nonlocal treatment of the exchange and correlation is necessary in order to represent the correct magnetization, the H-graphene interaction, and thus to build accurate potential energy surfaces for dynamical studies.

## ACKNOWLEDGMENTS

The authors thank the NOTUR consortium for providing computational resources. S.C. acknowledges the University of Oslo for the hospitality during his stay and Rocco Martinazzo for the many valuable comments. E.F.-L. would like to acknowledge the Norwegian Research Council for funding.

\*simone.casolo@unimi.it

- <sup>1</sup>A. H. Castro Neto, F. Guinea, N. M. R. Peres, K. S. Novoselov, and A. K. Geim, *Rev. Mod. Phys.* **81**, 109 (2009).
- <sup>2</sup>P. Avouris, Z. Chen, and V. Perebeinos, *Nat. Nanotechnol.* **2**, 605 (2007).
- <sup>3</sup>K. I. Bolotin, K. J. Sikes, Z. Jiang, M. Klima, G. Fudenberg, J. Hone, P. Kim, and H. L. Stormer, *Solid State Commun.* **146**, 351 (2008).
- <sup>4</sup>F. Schedin, A. K. Geim, S. V. Morozov, E. W. Hill, P. Blake, M. I. Katsnelson, and K. S. Novoselov, *Nat. Mater.* **6**, 652 (2007).
- <sup>5</sup>K. Novoselov, *Nat. Mater.* **6**, 720 (2007).
- <sup>6</sup>L. Jeloica and V. Sidis, *Chem. Phys. Lett.* **300**, 157 (1999).
- <sup>7</sup>X. Sha and B. Jackson, *Surf. Sci.* **496**, 318 (2002).
- <sup>8</sup>S. Casolo, O. M. Løvvik, R. Martinazzo, and G. F. Tantardini, *J. Chem. Phys.* **130**, 054704 (2009).
- <sup>9</sup>L. Hornekær, Ž. Šljivančanin, W. Xu, R. Otero, E. Rauls, I. Stensgaard, E. Lægsgaard, B. Hammer, and F. Besenbacher, *Phys. Rev. Lett.* **96**, 156104 (2006).
- <sup>10</sup>L. Hornekær, E. Rauls, W. Xu, Ž. Šljivančanin, R. Otero, I. Stensgaard, E. Lægsgaard, B. Hammer, and F. Besenbacher, *Phys. Rev. Lett.* **97**, 186102 (2006).
- <sup>11</sup>D. W. Boukhvalov, M. I. Katsnelson, and A. I. Lichtenstein, *Phys. Rev. B* **77**, 035427 (2008).
- <sup>12</sup>L. Schlapbach and A. Züttel, *Nature (London)* **414**, 353 (2001).
- <sup>13</sup>J. Küppers, *Surf. Sci. Rep.* **22**, 249 (1995).
- <sup>14</sup>R. J. Gould and E. E. Salpeter, *Astrophys. J.* **138**, 393 (1963).
- <sup>15</sup>D. Hollenbach and E. E. Salpeter, *J. Chem. Phys.* **53**, 79 (1970).
- <sup>16</sup>G. Kresse and J. Hafner, *Phys. Rev. B* **49**, 14251 (1994).
- <sup>17</sup>G. Kresse and J. Furthmüller, *Phys. Rev. B* **54**, 11169 (1996).
- <sup>18</sup>J. P. Perdew, K. Burke, and M. Ernzerhof, *Phys. Rev. Lett.* **77**, 3865 (1996).
- <sup>19</sup>P. E. Blöchl, *Phys. Rev. B* **50**, 17953 (1994).
- <sup>20</sup>G. Kresse and D. Joubert, *Phys. Rev. B* **59**, 1758 (1999).
- <sup>21</sup>J. C. Slonczewski and P. R. Weiss, *Phys. Rev.* **109**, 272 (1958).
- <sup>22</sup>M. Inui, S. A. Trugman, and E. Abrahams, *Phys. Rev. B* **49**, 3190 (1994).
- <sup>23</sup>E. H. Lieb, *Phys. Rev. Lett.* **62**, 1201 (1989).
- <sup>24</sup>T. O. Wehling, M. I. Katsnelson, and A. I. Lichtenstein, *Phys. Rev. B* **80**, 085428 (2009).
- <sup>25</sup>P. W. Anderson, *Phys. Rev.* **124**, 41 (1961).
- <sup>26</sup>D. M. Newns, *Phys. Rev.* **178**, 1123 (1969).
- <sup>27</sup>M. Lindenblatt and E. Pehlke, *Phys. Rev. Lett.* **97**, 216101 (2006).
- <sup>28</sup>M. S. Miziałinski, D. Bird, M. Persson, and S. Holloway, *Surf. Sci.* **602**, 2617 (2008).
- <sup>29</sup>A. J. Cohen, P. Mori-Sánchez, and W. Yang, *Science* **321**, 792 (2008).
- <sup>30</sup>O. Gritsenko, B. E. P. R. T. Schipper, and E. J. Baerends, *J. Phys. Chem. A* **104**, 8558 (2000).
- <sup>31</sup>Y. Zhang and W. Yang, *J. Chem. Phys.* **109**, 2604 (1998).
- <sup>32</sup>P. Mori-Sánchez, A. J. Cohen, and W. Yang, *Phys. Rev. Lett.* **102**, 066403 (2009).
- <sup>33</sup>K. Burke, J. P. Perdew, and M. Ernzerhof, *J. Chem. Phys.* **109**, 3760 (1998).
- <sup>34</sup>J. P. Perdew, A. Savin, and K. Burke, *Phys. Rev. A* **51**, 4531 (1995).
- <sup>35</sup>J. P. Perdew, R. G. Parr, M. Levy, and J. L. Balduz, Jr., *Phys. Rev. Lett.* **49**, 1691 (1982).
- <sup>36</sup>J. P. Perdew, A. Ruzsinszky, G. I. Csonka, O. A. Vydrov, G. E. Scuseria, V. N. Staroverov, and J. Tao, *Phys. Rev. A* **76**, 040501(R) (2007).
- <sup>37</sup>P. Mori-Sánchez, A. J. Cohen, and W. Yang, *Phys. Rev. Lett.* **100**, 146401 (2008).
- <sup>38</sup>A. Ruzsinszky, J. P. Perdew, G. I. Csonka, O. A. Vydrov, and G. E. Scuseria, *J. Chem. Phys.* **125**, 194112 (2006).
- <sup>39</sup>M. Marsman, J. Paier, A. Stroppa, and G. Kresse, *J. Phys.: Condens. Matter* **20**, 064201 (2008).
- <sup>40</sup>C. Adamo and V. Barone, *J. Chem. Phys.* **110**, 6158 (1999).
- <sup>41</sup>A. J. Cohen, P. Mori-Sánchez, and W. Yang, *Phys. Rev. B* **77**, 115123 (2008).
- <sup>42</sup>S. L. Dudarev, G. A. Botton, S. Y. Savrasov, C. J. Humphreys, and A. P. Sutton, *Phys. Rev. B* **57**, 1505 (1998).
- <sup>43</sup>M. Cococcioni and S. de Gironcoli, *Phys. Rev. B* **71**, 035105 (2005).
- <sup>44</sup>T. G. Pedersen, *Phys. Rev. B* **69**, 075207 (2004).
- <sup>45</sup>T. G. Pedersen, C. Flindt, J. Pedersen, N. A. Mortensen, A. P. Jauho, and K. Pedersen, *Phys. Rev. Lett.* **100**, 136804 (2008).